Electric- and magnetic-field-induced evolution of transport windows in a vertical quantum dot

B. Szafran,* S. Bednarek, and J. Adamowski
Faculty of Physics and Nuclear Techniques, University of Mining and Metallurgy (AGH), Kraków, Poland
(Received 6 August 2001; published 21 December 2001)

A theoretical description is presented for the quantum Coulomb blockade observed in a vertical gated quantum dot. We have applied a self-consistent approach to a solution of the Poisson-Schrödinger problem, which takes into account the electrostatics of the entire nanostructure. The conditions under which the Coulomb blockade and the transport windows appear in the current-voltage characteristics of the nanodevice are determined as functions of the external magnetic field and the potentials applied to the electrodes. We have discussed the magnetic-field induced ground-state transformations in the system of electrons confined in the quantum dot and their consequences for the measured characteristics of the nanodevice. The results of the present calculations are in a good agreement with the experimental data.

DOI: 10.1103/PhysRevB.65.035316 PACS number(s): 73.21.−b, 73.63.−b

I. INTRODUCTION

In a semiconductor quantum dot (QD),[1] the movement of charge carriers is limited in all the three dimensions. As a consequence, the energy of electrons confined in the QD takes on discrete values. The confined states can be studied by the transport spectroscopy,[2] which measures the current resulting from the single-electron tunneling via the QD. The flow of the single-electron current through the QD is blocked if there appears a mismatch between the electrochemical potential of the leads and the chemical potential of the QD. This effect, called the Coulomb blockade,[3] in large QD's (with size of several hundreds nanometers) can be explained by a classical-capacitor model, as a consequence of a discrete character of the electron charge. In small QD's the energy spacings between the size-quantized levels are larger (several meV) and are comparable with the energy of the Coulomb interaction between the confined electrons. In this case, the quantum effects, e.g., the discrete spectrum of electron energy levels, are observed as an unequal spacing between the current peaks and are interpreted in terms of the shell filling.[4] The shell filling has been first observed by Tarucha *et al.*[4] and Kouwenhoven *et al.*[5] in the current-voltage characteristics of the vertical gated QD's. The nanodevice used in these experiments was fabricated[6] from the planar heterostructure made of *n*-GaAs/AlGaAs/InGaAs/AlGaAs/*n*-GaAs layers, which were etched to form a pillar and surrounded by a ring-shaped Schottky gate. The application of the gated vertical QD allowed the authors[4,5] to perform very accurate measurements and discover the quantum phenomena in the electron transport.

The fascinating properties of the vertical QD[4,5,7] have inspired several attempts[8–13] of theoretical interpretation of the experimental data. The authors[8–11] used confinement potentials, which were assumed to be independent of the voltages applied to the gate, source, and drain electrodes, and the number of electrons confined in the QD. In fact, because of the complex electrostatics of the nanodevice, the confinement potential of the QD depends on the applied voltages and the number of the confined electrons.[14,15] Due to the neglect of this dependence, the authors[8–11] were unable to compare directly their theoretical results with the experimentally measured[4,5] current-voltage characteristics of the vertical QD and obtained only a qualitative interpretation of the experimental data.[4,5] The confinement potential was calculated from the Poisson equation in Ref. 12 for a model nanostructure with the different shape and geometry than the nanodevice studied by Tarucha *et al.*[4] and Kouwenhoven *et al.*[5] In the recent paper, Matagne *et al.*[13] investigated the electronic properties of the QD's with a geometry similar to the device of Tarucha[4] by solving the Schrödinger-Poisson problem self-consistently for zero source-drain voltage in the absence of external magnetic field.

In our previous paper,[14] we have solved the Poisson-Schrödinger problem for the entire nanodevice[4] and obtained a very good quantitative agreement of calculated results with the experimental data.[4,5] Namely, we have calculated the values of the gate voltage, which correspond to the subsequent current peaks for the zero drain-source voltage, and determined their evolution in the external magnetic field. Moreover, we have reproduced the shape of the six lowest Coulomb diamonds, i.e., the regions of the Coulomb blockade, as functions of the gate voltage and drain-source voltage. In a recent development[15] of the model,[14] we have included the nominal values of the material parameters of the nanostructure.[4] As a result, we have obtained[15] the shapes, positions, and sizes of the 12 Coulomb diamonds in a very good agreement with experiment.[5]

In the present paper, we study the Coulomb blockade in the vertical QD subjected to external electric and magnetic fields. In particular, we perform the calculations for the nonzero drain-source voltage. The application of the drain-source voltage creates in the QD the component of electric field parallel to the axis of the device. The reaction of the confined electron system on this electric field gives information about the voltage-to-energy conversion factor.[4] On the other hand, the measurements[4,5] of the current-voltage characteristics in the external magnetic field yield an information about the symmetry of the confined electron states, the localization of the confined charge, and the relative strength of the electron-electron interaction. Therefore, the joint effect of the source-drain voltage and the external magnetic field on the electron system confined in the QD is one of the most interesting characteristics of the nanodevice, which—to the best

of our knowledge, has not been studied until now in theoretical papers. The calculations of these effects presented in this paper have been performed in the framework of the theory of the vertical QD described in Refs. 14 and 15 with the nominal values of the nanostructure parameters.[15] The present paper is organized as follows: in Sec. II, we present the theoretical model, Sec. III contains results of calculations and their discussion, and Sec. IV contains a summary.

II. THEORY

The theoretical approach elaborated in Refs. 14, 15 is based on the self-consistent solution of the Poisson and Schrödinger equations which takes into account the modulated doping, the coupling between the electrons confined in the dot and the ionized donors and all the applied voltages. The Hamiltonian for N electrons confined in the QD is taken on in the form

$$H=\sum_{i=1}^{N} h(\mathbf{r}_i)+\frac{e^2}{4\pi\varepsilon_0\varepsilon_\infty}\sum_{\substack{i,j=1\\ i>j}}^{N}\frac{1}{r_{ij}}, \tag{1}$$

where

$$h(\mathbf{r})=-\frac{\hbar^2}{2m^*}\nabla^2+U_{\mathrm{db}}(z)-e\varphi(\mathbf{r}) +\frac{1}{8}m^*\omega_c^2(x^2+y^2)+\frac{1}{2}\hbar\omega_c l_z, \tag{2}$$

is the one-electron Hamiltonian, N is the number of excess electrons confined in the QD, e is the elementary charge ($e>0$), m^* is the electron effective band mass, ε_∞ is the high frequency dielectric constant of the QD material, r_{ij} is the interelectron distance, $\omega_c=eB/m^*$ is the cyclotron frequency for magnetic field B, and l_z is the z-component angular-momentum operator. We adopt the effective mass of the $In_{0.05}Ga_{0.95}As$ alloy, i.e., $m^*=0.064m_{e0}$,[16] where m_{e0} is the electron rest mass, and the dielectric constant of GaAs $\varepsilon_\infty=11$. The spin Zeeman effect, which in GaAs is much smaller than the magnetic orbital effects, was neglected. The electrons are confined in the QD by the double-barrier AlGaAs/InGaAs heterostructure with potential energy $U_{\mathrm{db}}(z)$ and by the external electrostatic field with potential $\varphi(\mathbf{r})$, which is the solution of the Poisson equation.[14] Potential $\varphi(\mathbf{r})$ leads to the lateral confinement of the electrons in the QD.

The electrons confined in the QD interact with the ionized donors in the n-GaAs layers. We take this coupling into account by solving the Poisson-Schrödinger problem with use of the self-consistent procedure. As a result, we obtain potential $\varphi(\mathbf{r})$, which depends on the voltages applied to the gate (V_g) and drain (V_{ds}) as well as on the number (N) and the density of the electrons confined in the QD. We have solved the Poisson equation by the finite-difference relaxation method[14,15] and the Schrödinger equation by the unrestricted Hartree-Fock method.[15,17] The solution of the Poisson-Schrödinger problem yields the realistic three-dimensional profile of potential $\varphi(\mathbf{r})$ and N-electron ground-state energy E_N.

In the vertical QD,[4,5] a single electron can tunnel from the source to the drain via the N-electron state if chemical potential μ_N falls into the transport window, which is defined as the energy interval determined by the electrochemical potentials of both the electron reservoirs, i.e.,

$$\mu_{\mathrm{source}}\geqslant\mu_N\geqslant\mu_{\mathrm{drain}}. \tag{3}$$

The chemical potential of the N-electron system is calculated as follows: $\mu_N=E_N-E_{N-1}$. The electrochemical potential of the contact is defined as the highest occupied energy level of the corresponding electron reservoir. In the nanodevice,[4] the source and drain contacts, which are connected to the strongly doped n-GaAs layers, possess the Ohmic character. The measurements[4,5] were performed at the very low temperature (0.2 K). In this case, the electrochemical potential of the contacts can be identified with the donor energy level in the n-GaAs layers. The difference between the electrochemical potentials of the two reservoirs is controlled by the drain-source voltage, i.e.,

$$\mu_{\mathrm{source}}-\mu_{\mathrm{drain}}=eV_{\mathrm{ds}}. \tag{4}$$

If condition (3) is not fulfilled for any N, the flow of the source-drain current is blocked and the number of the electrons confined in the QD is fixed, which means that the Coulomb blockade appears. The energetic position of chemical potential μ_N of the confined electron system with respect to the drain and source electrochemical potentials can be tuned by the gate voltage. Thus, the number of electrons confined in the QD can be intentionally changed.

The magnetic field affects not only the energy of the QD confined electron system, but also energy E_D of the electron bound to a donor impurity, e.g., the electrochemical potential of the corresponding contact. In the range of the magnetic field applied, i.e., $B\in[0,8\,\mathrm{T}]$, this dependence is weak and has been taken into account by the perturbation method,[18] which leads to

$$E_D(B)=E_D(0)+\lambda B^2, \tag{5}$$

where $E_D(0)=-5.8\,\mathrm{meV}$ is the Si energy at zero magnetic field measured with respect to the conduction-band minimum and $\lambda=8.28\times10^{-3}\,[\mathrm{meV/T^2}]$. Let us note that even at low temperatures the electrons are not frozen out on the donor centers due to the considerable overlap between the weakly localized donor states in the doped GaAs layers.[4,5] Therefore, the small currents are possible via the overlapping donor impurity states.

The Schrödinger equation for the confined electron was solved with the unrestricted Hartree-Fock method with the one-electron wave-functions expanded in a variational basis

$$\psi_\nu(\mathbf{r})=\exp(-\beta z^2)\sum_{k=1}^{3}\sum_{i,j=0}^{i+j\leqslant4}c_{kij}^{\nu}x^iy^j \times\exp[-(\alpha/k)(x^2+y^2)], \tag{6}$$

where α and β are the nonlinear variational parameters, which describe the localization of the wave functions in the lateral and vertical directions, respectively. In this paper, we

consider the QD's confining up to five electrons and the magnetic-field range up to 8 T. The last value corresponds to a maximum-density droplet phase.[19–21] In this phase, the electrons are fully spin polarized and occupy subsequent states with the definite z component of the angular momentum. The upper bounds on summations on i and j in basis (6) has been chosen sufficiently large in order to construct the angular momentum eigenstates with $|m| \leqslant 4$, where m is the quantum number of the z component of the angular momentum. The iterations in the self-consistent Hartree-Fock calculations are carried out in a manner, which ensures that the one-electron wave functions are the eigenstates of the z-component angular-momentum operator. The formation of Wigner molecules, which can occur at higher magnetic field,[19–21] is not considered here.

In the present paper, the drain-source (bias) voltage has been included via the boundary conditions put on the electrostatic potential on the drain and source electrodes when calculating the electrostatic potential profile from the Poisson equation.[15] Due to the small voltage drop across the QD region, we assume that the charge density of the electrons confined in the QD is not deformed by the bias voltage (vertical electric field) [cf, Eq. (6)]. Let us estimate the potential-energy contribution originating from the bias-voltage drop across the QD for the considered bias regime, i.e., $0 \leqslant V_{\mathrm{ds}} \leqslant 3$ meV. For this purpose, we consider the electrostatics of the nanodevice. In the n-GaAs layers attached to the source and drain, the donor center becomes ionized if the potential energy of the electrostatic field exceeds the donor energy, i.e., the electrochemical potential of the corresponding lead. This leads to a formation of the positive space charge associated with the ionized donors.[15]

In such the way, the drain-source voltage is transferred into the neighborhood of the double-barrier heterostructure. As a result, the entire bias-voltage drop occurs in the region, that consists of the ionized part of the n-GaAs layers, the undoped GaAs spacer, and the AlGaAs/InGaAs double-barrier heterostructure. The estimated minimal thickness of this region is equal to the sum of the thicknesses of the two GaAs spacers and the AlGaAs/InGaAs double-barrier heterostructure, which gives $\sim$35 nm.[15] Hence, we have estimated that the change of the electron potential energy, which results from the voltage drop across the 12-nm-thick InGaAs QD layer, is $\sim$1 meV. For comparison, the energy spacing between the ground state and the first excited state of the quantized motion of the electron in the z direction is $\sim$80 meV. This justifies the neglect of the influence of the bias voltage on the electron wave functions inside the QD.

III. RESULTS AND DISCUSSION

A. Zero magnetic field

In order to understand the influence of the external magnetic field on the single-electron transport, we begin with the results for the zero-field limit. These results will also serve us for explaining the concept of a transport window, which is the main subject of the present work. Figure 1 shows the enlargement of the lower part ($N=1,...,6$) of the stability diagram, which is fully shown in Fig. 12 (Ref. 15). This

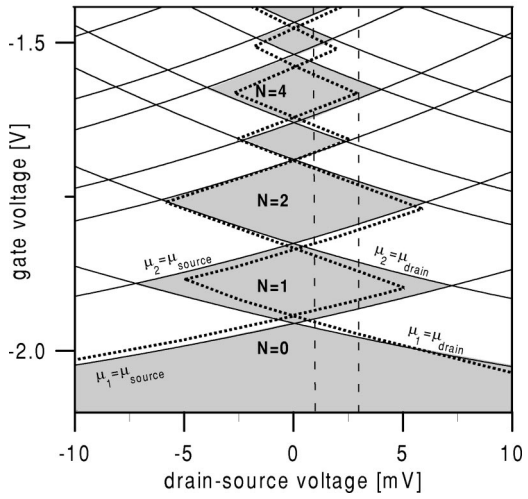

FIG. 1. Stability diagram with Coulomb diamonds and transport windows. Solid (dotted) curves show the calculated (measured) boundaries of the regions of the single-electron tunneling via the QD as functions of the gate voltage and drain-source voltage. The calculated chemical potential μ_N of the N-electron system is aligned with the electrochemical potentials of the source (μ_{source}) and drain (μ_{drain}) along the solid curves. The shaded areas are the regions of the Coulomb blockade, in which the number of the electrons confined in the QD is fixed and equal to N. The white areas correspond to the transport windows. The thin vertical lines mark the drain-source voltage values, for which the results in Figs. 2, 6, and 7 are displayed.

zoom enables us to present the details of small deviations of the calculated[15] and measured[4,5] data that are essential for the discussion of the results of the present paper. In Fig. 1, the solid lines correspond to the values of the gate and drain-source voltages, for which the chemical potential of N electrons is aligned with the electrochemical potential of one of the contacts, i.e., single-electron tunneling condition (3) is fulfilled (with the equality sign). If the voltages are swept across these lines, the transport windows are opened (when passing into the white areas in Fig. 1) and closed (when passing into the shaded areas). The shaded areas located near the $V_{\mathrm{ds}}=0$ show the calculated Coulomb diamonds. The white areas correspond to the voltages, for which a transport window is opened for at least one N. The thick dotted curves correspond to the borders of the Coulomb diamonds measured by Kouwenhoven *et al.*[5]

The positions, sizes, and shapes of the calculated Coulomb diamonds agree well with the experimental data.[5] The largest deviations from the experimental data occur for the first and fourth diamond, which are slightly larger than the measured Coulomb diamonds (cf., Fig. 1). These deviations can be attributed to the neglect of the electron-electron correlation in the Hartree-Fock method applied in the present paper. The electron-electron correlation appears for the second electron confined in the QD. We have estimated[22] the correlation energy of the two-electron system in the vertical QD to be of the order of 1 meV. Therefore, chemical potential μ_2, that determines the upper boundary of the first Coulomb diamond, is slightly overestimated. It seems that the neglect of the correlation is directly responsible for the small

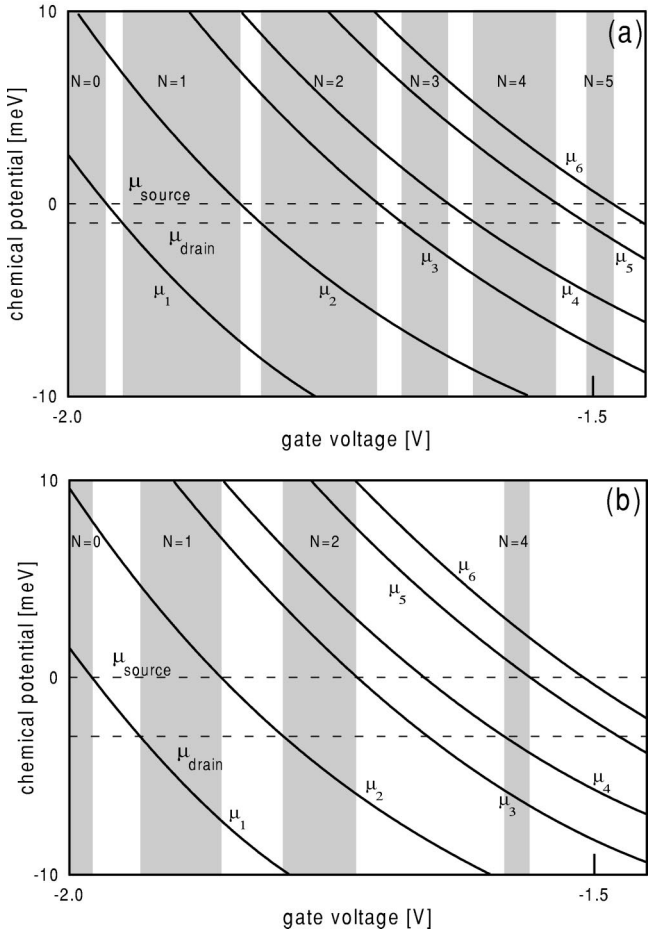

FIG. 2. Chemical potentials μ_N (solid lines) of the N-electron system confined in the QD as functions of the gate voltage for drain-source voltage $V_{ds}=1$ mV (a) and $V_{ds}=3$ mV (b). The horizontal dashed lines show the electrochemical potentials of the source and drain. The shaded areas (Coulomb-blockade regions) correspond to the gate-voltage regimes, for which all the transport windows are closed. N is the number of the electrons confined in the QD. The white areas correspond to the voltages, for which at least one transport window is opened.

discrepancy between the theory and experiment for the first Coulomb diamond in Fig. 1. It is known[22] that the Hartree-Fock method works better for the states with the higher values of the total spin. In the case of the fourth Coulomb diamond in Fig. 1, this is the four-electron state, in which the second electronic shell is half filled and the total spin takes on the maximal value. The boundaries of the fourth Coulomb diamond are determined by μ_4 and μ_5, which are evaluated with use of ground-state energies E_3, E_4, and E_5. In the Hartree-Fock approach, energy E_4 is calculated with the higher precision than E_3 and E_5, which leads to an enlargement of the fourth Coulomb diamond calculated by this method. Therefore, we can ascribe the obtained overestimation of the area of the fourth Coulomb diamond to the neglect of the correlation in the Hartree-Fock method.

For the small drain-source voltage condition (3) is fulfilled in narrow intervals of V_g only. Then, the current-gate voltage characteristics possesses a form of a series of sharp

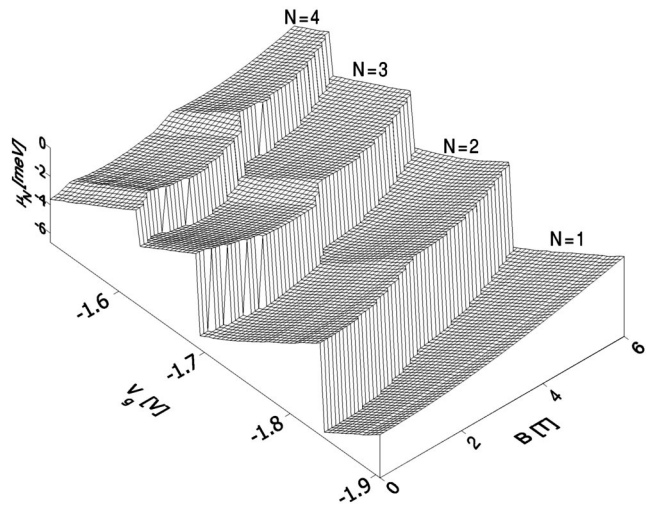

FIG. 3. Chemical potential μ_N of the N-electron QD as a function of magnetic-field B, gate voltage V_g, and number N of electrons confined in the QD for drain-source voltage $V_{ds}=0$. Zero on the energy scale corresponds to the Fermi energy of the source and drain.

peaks[4] and the corresponding transport windows are narrow. If the drain-source voltage increases, the transport windows become wider and the Coulomb-blockade regions shrink. The dependence of the chemical potentials on the gate voltage for $N=1,...,6$ electrons is shown in Fig. 2(a) for $V_{ds}=1$ mV and in Fig. 2(b) for $V_{ds}=3$ mV. These voltages are marked by the vertical dashed lines on Fig. 1. The electrochemical potentials of the source and drain are marked by the horizontal dashed lines on Figs. 2(a) and 2(b). The values of the gate voltage, for which μ_N falls in between these lines, corresponds to the transport window (white areas) with the single-electron tunneling via the N-electron state of the QD. For $V_{ds}=1$ mV the transport windows are rather thin [Fig. 2(a)] and do not overlap. Therefore, for $V_{ds}=1$ mV the Coulomb blockade (shaded areas in Fig. 2) can be observed for each N. For $V_{ds}=3$ mV [Fig. 2(b)] the transport windows become thicker and start to overlap. For example, there is an overlap between the transport windows corresponding to $N=3$ and 4, which leads to a disappearance of the Coulomb blockade for the three-electron QD at $V_{ds}=3$ mV. Due the similar reason, the Coulomb-blockade electrons is not observed for the five electrons in the QD [Fig. 2(b)].

B. Effect of magnetic field

The application of the external magnetic field shifts the current peaks on the gate-voltage scale and leads to the magnetic-field-induced transformations of the N-electron ground state. For the small bias these effects are illustrated in Figs. 3 and 4. Figure 3 shows the number of electrons, which fill the QD, and their chemical potential calculated at zero bias as functions of the magnetic field and gate voltage. For $V_{ds}=0$ the QD states are filled by the excess electrons up to the common electrochemical potential of the source and drain, i.e., the Fermi level (zero on the energy scale). The steps in Fig. 3 correspond to the change of the number of

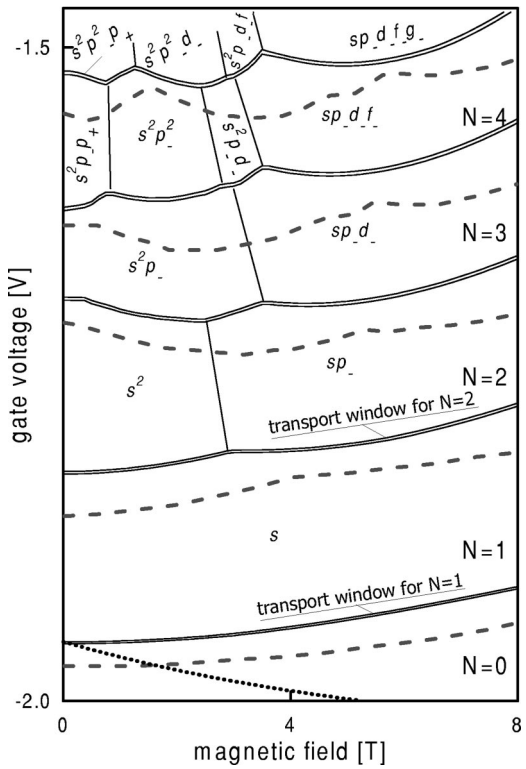

FIG. 4. Transport windows as functions of the gate voltage and magnetic field for $V_{ds}=0.1$ mV. Solid (dashed) curves show the calculated (measured) values of the gate voltage and magnetic field, for which the single electrons tunnel through the QD. N denotes the number of the QD-confined electrons. In the Coulomb-blockade regions, N is fixed, while in the transport windows, the number of the electrons in the QD fluctuates as follows: $N-1\rightarrow N\rightarrow N-1\cdots$. The ground-state orbital configurations are labeled by symbols *s*, *p*, *d*, *f*, and *g*, which denote the quantum numbers $m=0$, 1, 2, 3, and 4, respectively, the sign ($\pm$) in the subscript is the sign of the *z* component of the angular momentum. The regions corresponding to the different ground-state orbital configurations are separated by the thin solid lines. All the states possess the maximum allowed value of the *z* component of the total spin. The dotted curve shows the results for the tunneling of the first electron via the QD obtained under the hypothesis that the Fermi level is identified with the GaAs lowest energy Landau level.

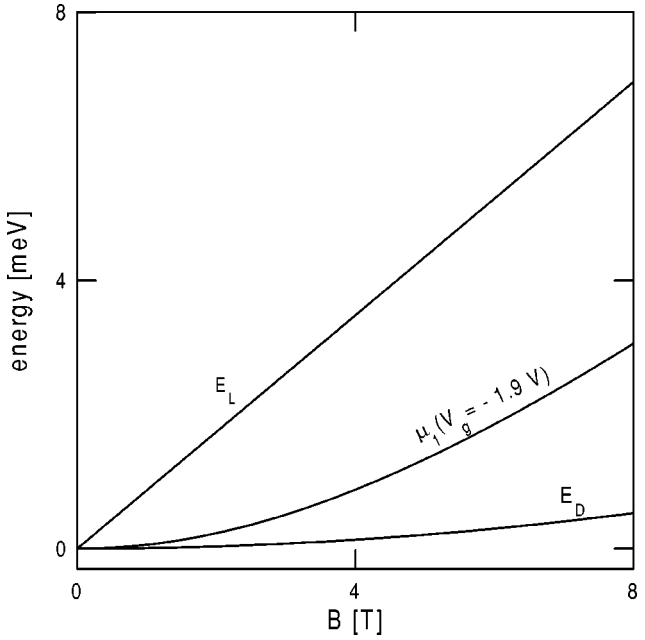

FIG. 5. Donor energy (E_D), GaAs lowest Landau level (E_L), and chemical potential (μ_1) as functions of magnetic field B. Each quantity is measured with respect to its value taken at $B=0$.

electrons confined in the QD by one, i.e., the single-electron charging (or discharging) of the QD. The cusps visible along the steps appear for the fixed number of the QD confined electrons and correspond to the magnetic-field-induced transformations of the N-electron ground state. The results of Fig. 3 can be translated into the positions of the single-electron current peaks on the V_g-B plane, which are shown in Fig. 4. Figure 4 displays the dependence of the gate voltage, which corresponds to the boundaries of the transport windows, on the magnetic field for the small drain-source voltage ($V_{ds}=0.1$ mV). At this bias, the Coulomb blockade occurs in the major part of the V_g-B plane. In Fig. 4, we have marked number N of the electrons confined in the QD and the orbital configurations of the N-electron ground states. The one-electron orbitals are labeled as follows: symbols *s*, *p*, *d*, *f*, and *g* correspond to quantum numbers $m=0$, 1, 2, 3, and 4, respectively, and the sign in the subscript denotes the sign of the *z* component of the angular momentum. The ground states correspond to the maximal value of the *z* component of the total spin that is allowed for a given spatial configuration. Since the N-electron ground-state energy E_N appears twice in single-electron tunneling condition (3), each ground-state transformation can be observed two times on the boundary of the transport window, that corresponds to the tunneling via the N- and $(N+1)$-electron state. In Fig. 4, the points corresponding to the same ground-state transformation are connected by the thin straight lines. If the gate voltage increases, the same ground-state transformation appears at the lower magnetic field (the slope of the thin lines is negative). This effect results from the change of the lateral confinement potential with the gate voltage.[14,15] If the gate voltage increases, the confinement potential flattens and the electron system becomes more weakly localized in the QD. For the weakly localized electron system the relative influence of the magnetic field is stronger, which shifts the ground-state transformation towards the weaker magnetic field. This effect is experimentally observed,[4,5] but cannot be explained in the framework of the models, that assume the fixed, gate-voltage independent, confinement potential.[8–12] The low-field shift of the ground-state transformation for the same number of electrons can only be understood, if we take into account the influence of the gate voltage on the confinement potential.[14,15]

For $B=0$ the N-electron ground-state spin-orbital configuration can be predicted by Hund's rule. In the opposite limit, i.e., for the strong magnetic field, the ground state is completely spin polarized. For the intermediate magnetic field the ground-state transformations (''phase transitions'') appear. The magnetic-field-induced phase transitions result from the competition between the Coulomb interaction, ki-

netic energy, and orbital Zeeman interaction. If the magnetic field increases, the phase transition leads to a maximization of the z components of both the total spin and total angular momentum. With the exception of the first (low-field) transformation for $N=4$, in all the transformations marked in Fig. 4, the Coulomb-interaction contribution is decreased. During the ground-state transformation in the four-electron system at $B \simeq 1$ T, Hund's rule is broken and the Coulomb repulsion between the p electrons increases.

In Fig. 4, the dashed curves display the experimental data.[5] The present theoretical results well reproduce the shapes of the experimental curves. However, the values of the critical fields, for which the ground state transforms into the high-spin state with the lower Coulomb interaction, are underestimated by about 30–40%. On the other hand, the critical field, at which the Hund-rule breaking transformation appears for the four electrons, is slightly overestimated. In this transformation, in the four-electron system, the z component of the total spin decreases and the Coulomb interaction increases. We ascribe these deviations to the inaccuracy of the Hartree-Fock method used in the present paper. We have found[22] that the Hartree-Fock method yields more accurate results for the spin-polarized states than for the spin-unpolarized states. Therefore, the Hartree-Fock approach favors the spin polarization of the ground state, which leads to too small values predicted for the corresponding critical fields. A better agreement between the calculated and measured values of the critical magnetic fields should be obtained, if the energy of the Coulomb interaction in the confined electron system was smaller. In our previous paper,[14] we have presented the results of the calculations with the electron-electron interaction screened by low-frequency dielectric constant $\varepsilon_s = 13.2$, which is larger than high-frequency constant ε_∞ used in the present paper. However, the interaction between the weakly localized electrons should rather be screened by the high-frequency dielectric constant.[23] Moreover, we have checked[15] that the application of the static dielectric constant to the screening of the interaction between the electrons confined in the QD does not allow for a description of the electrostatics of the nanodevice for the higher number of electrons ($N>6$). This description is possible, if we apply the screening via the high-frequency dielectric constant.[15] Therefore, in this work, we have adopted ε_∞ as well as all the other material and nanodevice parameters given in Ref. 15 without any change.

The external magnetic field shifts the Fermi level. In the leads, this shift is consistent with the shift of the Landau level in the metal and—for the magnetic fields considered in

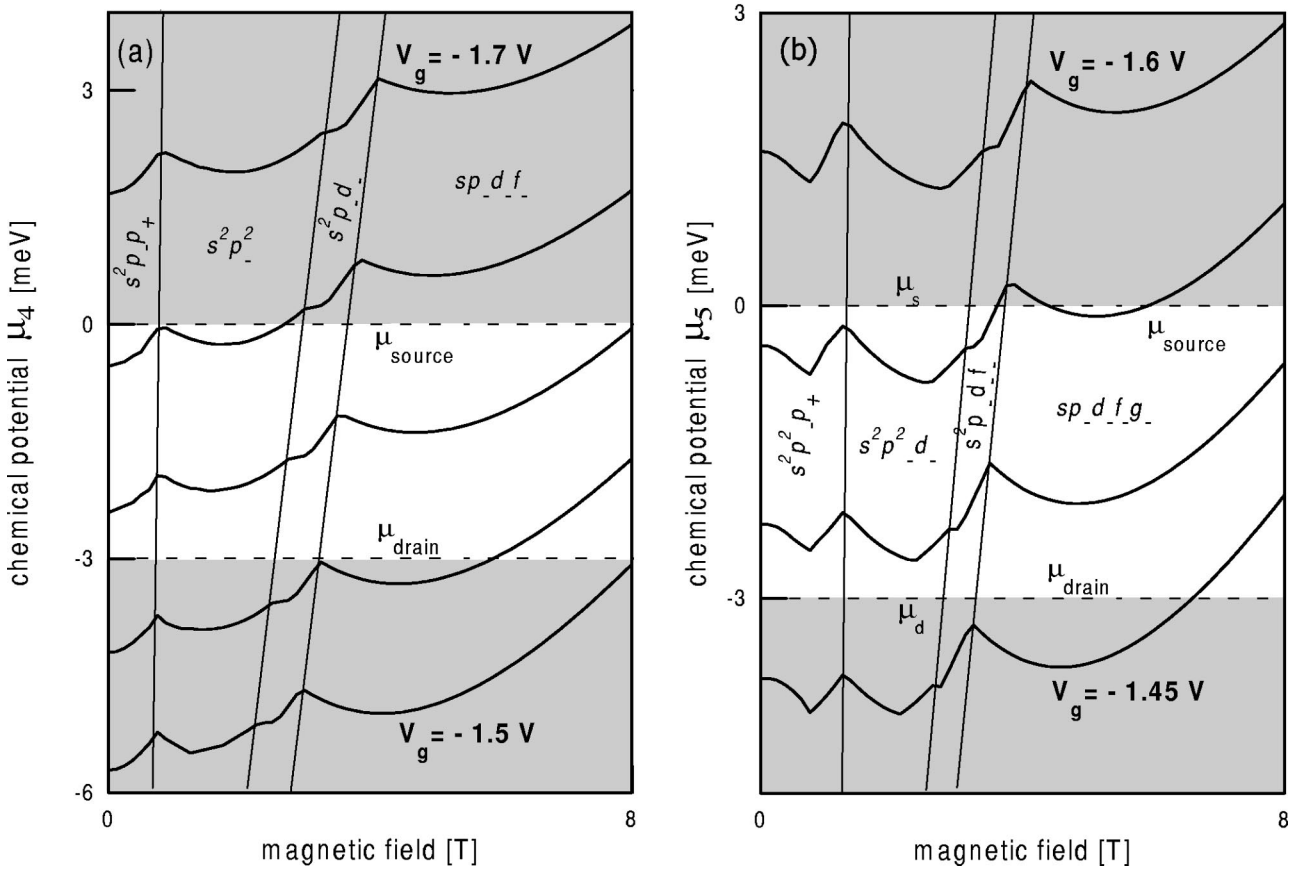

FIG. 6. Chemical potential of N electrons confined in the QD for $N=4$ (a) and $N=5$ (b) as a function of the magnetic field and gate-voltage V_g for drain-source voltage $V_{ds}=3$ mV. The gate voltage changes from -1.7 to -1.5 V in (a) and from -1.45 to -1.6 V in (b) with step 0.05 V. The horizontal dashed lines show the electrochemical potentials of the source and drain. The white (shaded) areas correspond to the open (closed) transport windows. The thin solid lines separate the regions with the different ground-state orbital configurations.

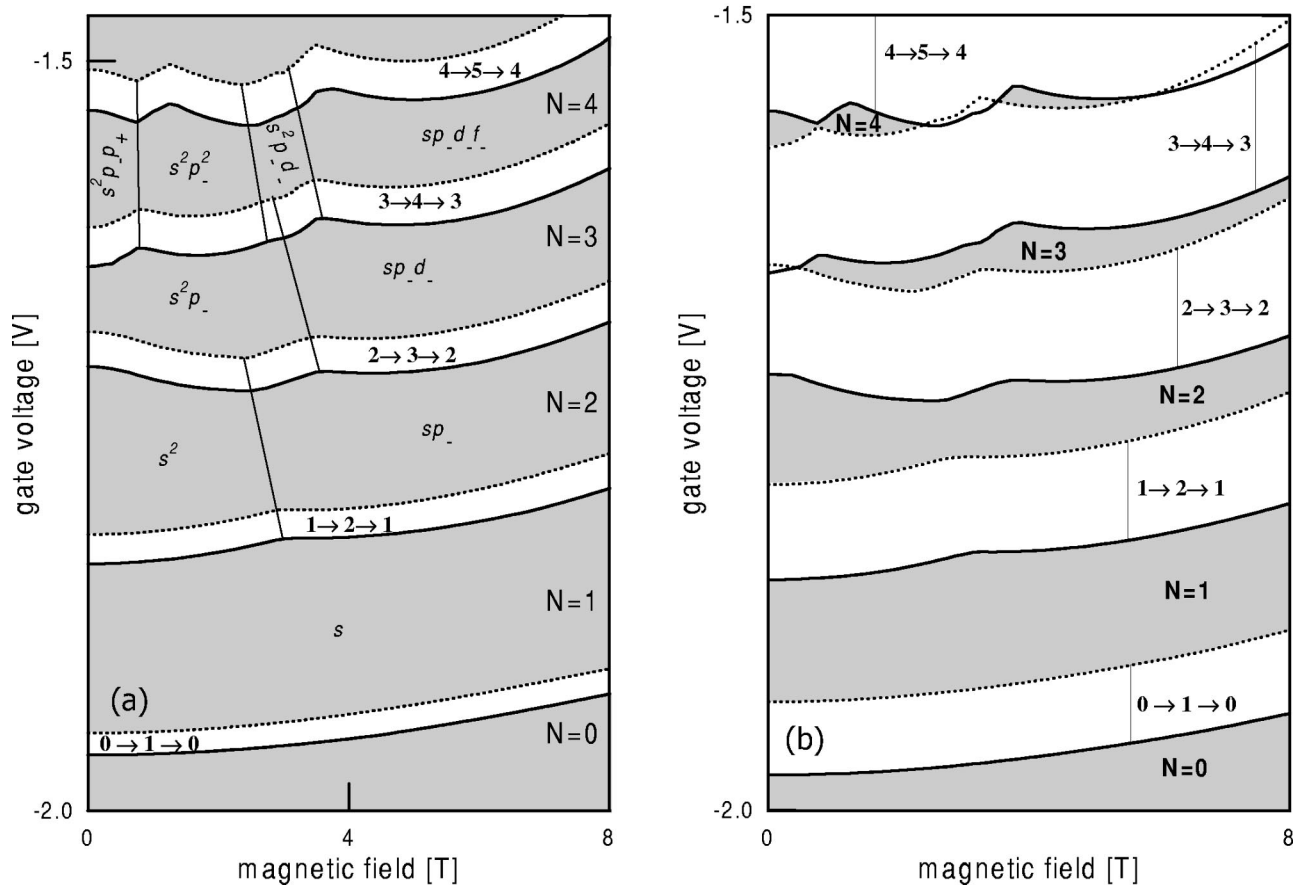

FIG. 7. Transport windows (white areas) and Coulomb-blockade regions (shaded areas) as functions of the gate voltage and magnetic field for drain-source voltage $V_{ds}=1$ mV (a) and $V_{ds}=3$ mV (b). Solid (dotted) lines show the values of the gate voltage and magnetic field, for which the chemical potential of the N-electron system confined in the QD is aligned with the electrochemical potentials of the drain (source). The values corresponding to the same ground-state transformation in the N-electron system confined in the QD are connected with the thin solid lines. In plot (a), the N-electron ground-state orbital configurations are given. In plot (b), the vertical thin lines connect the boundaries of the subsequent transport windows. The symbols in the transport windows show how the number of electrons in the QD fluctuates during the single-electron tunneling.

the present paper—is negligibly small due to the much larger effective electron mass[24] in comparison to the conduction-band electron mass in GaAs. In the Ohmic contacts between the leads and the n-GaAs layers, the Fermi levels in the metal and semiconductor equalize with each other. We assume that the semiconductor Fermi level is aligned with the donor impurity level, which changes with the magnetic field according to parabolic formula (5). We note that—in the vertical QD with the double-barrier heterostructure[4,5] the Fermi level cannot be identified with the lowest Landau level (E_L) in GaAs, which is a linear function of the magnetic field, i.e., $E_L=\hbar eB/2m^*$. For GaAs the coefficient in this formula is relatively large; namely, $\hbar e/2m^*=0.87$ meV/T. Therefore, the lowest Landau level grows with the magnetic field much faster than the donor impurity level and also faster that the chemical potentials of the electrons confined in the QD (Fig. 5). If the Fermi level were identified with the lowest Landau level, the fulfillment of single-electron tunneling condition (3) would require the considerable decrease of the gate voltage, i.e., the gate voltage should be more negative. Therefore, the gate voltage corresponding to all the current peaks would rapidly drop towards more negative values with the increasing magnetic field. This hypothetical effect is illustrated for the first peak by the dotted curve in Fig. 4. We see that the magnetic-field dependence of the current peaks would be completely different from that observed by Tarucha *et al.*[4] and Kouwenhoven *et al.*[5] The results of Figs. 4 and 5 support the present identification of the Fermi level with the donor impurity level.

The magnetic-field dependence of the chemical potential for $N=4$ and 5 electrons in the QD is displayed in Figs. 6(a) and 6(b) for $V_{ds}=3$ mV and for the values of the gate voltage, which changes with the 50-mV step. In Figs. 6, the horizontal dashed lines correspond to the electrochemical potentials of the source and drain. The regions corresponding to different ground-state orbital configurations are separated by the thin straight lines. The gate-voltage dependence of the critical magnetic field for the phase transitions is approximately linear. In Figs. 6(a) and 6(b), the white areas correspond to the transport windows for the single-electron tunneling via the four-electron QD states and the gray areas correspond to the values of the gate voltage and magnetic

field, for which the transport windows are closed. We see that the magnetic field not only changes the ground-state symmetry, but also causes the opening and closing of the transport windows and in this way changes the number of the electrons confined in the QD. Moreover, the gate voltage that also controls the number of the confined electrons can change the ground state of the confined system due to its influence on the lateral confinement potential. In particular, the gate voltage can change the spin of the system of electrons confined in the QD.[25]

The boundaries between the Coulomb-blockade regions and transport windows are plotted on the V_g-B plane in Figs. 7(a) and 7(b) for $V_{ds}=1$ and 3 mV, respectively. The solid (dotted) curves correspond to the values of the gate voltage and magnetic field, for which chemical potential μ_N is aligned with the electrochemical potential of the drain (source). In the white (gray) areas of Figs. 7(a) and 7(b), the transport windows are opened (closed). In the Coulomb-blockade regime, the number of the electrons confined in the QD is fixed. The transport windows are labeled as follows: $N-1\rightarrow N\rightarrow N-1$, which shows how the number of the electrons in the QD oscillates when the single electrons tunnel via the QD. For $V_{ds}=3$ mV [Fig. 7(b)] the Coulomb-blockade regions are thin, which results from the overlap of the transport windows [cf., Fig. 2(b)]. The results of Fig. 7(b) compared with the experimental data (Fig. 4 in Ref. 5) show a reasonable agreement with experiment. However, the calculated Coulomb-blockade region for $N=4$ is somewhat larger than that measured. This discrepancy results from the overestimation of the size of the fourth diamond (cf., Fig. 1) discussed in Sec. III.A.

IV. SUMMARY

The self-consistent method for the solution of the Poisson-Schrödinger problem, elaborated in our previous papers,[14,15] has been applied to a description of the evolution of the windows of transport through the vertical gated QD in the external electric and magnetic fields. To the best of our knowledge, this is the first complete study of the joint effect of the gate voltage, the drain-source voltage, and the magnetic field on the few-electron system confined in the vertical gated QD. We have determined the conditions under which a single electron can tunnel through the QD and calculated the positions of the single-electron tunneling current peaks as functions of the gate voltage and the magnetic field. The present results are in a good agreement with the experimental data. We have also obtained magnetic-field-induced phase transitions in the electron system confined in the QD. However, the critical magnetic fields, at which the ground-state transformations into the states with the higher total spin occur, are underestimated. We have ascribed these deviations to the neglect of the electron-electron correlation in the Hartree-Fock method. The problem of the identification of the Fermi level in the vertical gated QD has been discussed.

ACKNOWLEDGMENTS

This paper has been partly supported by the Polish State Committee for Scientific Research (KBN) under Grant No. 5P03B 4920. One of the authors (B.S.) gratefully acknowledges the financial support from the Foundation for Polish Science (FNP).

*Email address: bszafran@agh.edu.pl

[1] *Nanotechnology*, edited by G. Timp (Springer Verlag, New York, 1999); L. Jacak, P. Hawrylak, and A. Wójs, *Quantum Dots* (Springer Verlag, Berlin, 1998).

[2] P. L. McEuen, E. B. Foxman, U. Meirav, M. A. Kastner, Y. Meir, N. S. Wingreen, and S. J. Wind, Phys. Rev. Lett. **66**, 1926 (1991); T. Schmidt, M. Tewordt, R. H. Blick, R. J. Haug, D. Pfannkuche, K. von Klitzing, A. Förster, and H. Lüth, Phys. Rev. B **51**, 5570 (1995).

[3] M. A. Kastner, Phys. Today **46(1)**, 24 (1993).

[4] S. Tarucha, D. G. Austing, T. Honda, R. J. van der Hage, and L. P. Kouwenhoven, Phys. Rev. Lett. **77**, 3613 (1996).

[5] L. P. Kouwenhoven, T. H. Oosterkamp, M. W. S. Danoesastro, M. Eto, D. G. Austing, T. Honda, and S. Tarucha, Science **278**, 1788 (1997).

[6] D. G. Austing, T. Honda, and S. Tarucha, Semicond. Sci. Technol. **11**, 388 (1996).

[7] L. P. Kouwenhoven, D. G. Austing, and S. Tarucha, Rep. Prog. Phys. **64**, 701 (2001).

[8] M. Eto, J. Appl. Phys. **36**, 3924 (1997).

[9] T. Ezaki, N. Mori, and C. Hamaguchi, Phys. Rev. B **56**, 6428 (1997).

[10] H. Tamura, Physica B **249–251**, 210 (1998).

[11] O. Steffens, M. Suhrke, and U. Rössler, Physica B **256–258**, 147 (1998).

[12] S. Nagaraja, P. Matagne, V. Y. Thean, J. P. Leburton, Y. H. Kim, and R. M. Martin, Phys. Rev. B **56**, 15 752 (1997).

[13] P. Matagne, J.-P. Leburton, J. Destine, and G. Cantraine, J. Computer Modeling Engineering Science **1**, 1 (2000).

[14] S. Bednarek, B. Szafran, and J. Adamowski, Phys. Rev. B **61**, 4461 (2000).

[15] S. Bednarek, B. Szafran, and J. Adamowski, Phys. Rev. B **64**, 195303 (2001).

[16] J. L. Shen, Y. D. Dai, Y. F. Chen, S. Z. Lee, Phys. Rev. B **51**, 17 648 (1995).

[17] S. Bednarek, B. Szafran, and J. Adamowski, Phys. Rev. B **59**, 13 036 (1999).

[18] B. Szafran, J. Adamowski, and S. Bednarek, Phys. Rev. B **61**, 1971 (2000).

[19] T. H. Oosterkamp, J. W. Janssen, L. P. Kouwenhoven, D. G. Austing, T. Honda, and S. Tarucha, Phys. Rev. Lett. **82**, 2931 (1999).

[20] H. M. Muller and S. E. Koonin, Phys. Rev. B **54**, 14 532 (1996).

[21] S. M. Reimann, M. Koskinen, M. Manninen, and B. R. Mottelson, Phys. Rev. Lett. **83**, 3270 (1999).

[22] B. Szafran, J. Adamowski, and S. Bednarek, Physica E (Amsterdam) **5**, 185 (2000).

[23] S. Bednarek and J. Adamowski, Phys. Rev. B **57**, 14 729 (1998).

[24] J. Smoliner, R. Heer, and G. Strasser, Phys. Rev. B **60**, R5137 (1999).

[25] G. Burkard, D. Loss, and D. P. DiVincenzo, Phys. Rev. B **59**, 2070 (1999).